

Improved Stack-Slide Searches for Gravitational-Wave Pulsars

Curt Cutler,^{*} Iraj Gholami,[†] and Badri Krishnan[‡]

Max-Planck-Institut für Gravitationsphysik, Albert-Einstein-Institut, Am Mühlenberg 1, D-14476 Golm, Germany

(Dated: May 17, 2005)

We formulate and optimize a computational search strategy for detecting gravitational waves from isolated, previously-unknown neutron stars (that is, neutron stars with unknown sky positions, spin frequencies, and spin-down parameters). It is well known that fully coherent searches over the relevant parameter-space volumes are not computationally feasible, and so more computationally efficient methods are called for. The first step in this direction was taken by Brady&Creighton (2000), who proposed and optimized a two-stage, stack-slide search algorithm. We generalize and otherwise improve upon the Brady-Creighton scheme in several ways. Like Brady&Creighton, we consider a stack-slide scheme, but here with an arbitrary number of semi-coherent stages and with a coherent follow-up stage at the end. We find that searches with three semi-coherent stages are significantly more efficient than two-stage searches (requiring about 2–5 times less computational power for the same sensitivity) and are only slightly less efficient than searches with four or more stages. We calculate the signal-to-noise ratio required for detection, as a function of computing power and neutron star spin-down-age, using our optimized searches.

PACS numbers: 04.80.Nn, 95.75.Pq, 97.60.Gb

I. INTRODUCTION

In analyzing data from Earth-based and space-based gravitational-wave (GW) detectors, we will be computationally limited in performing certain types of searches—especially searches for long-lived signals described by several unknown parameters. For such signals, the number of templates signals required to discretely cover the parameter space (at useful resolution) typically increases rapidly as a function of the observation time. For ground-based detectors, such as LIGO, a well-known example is the search for nearly periodic GWs from unknown, isolated, rapidly rotating neutron stars (NSs). We will refer to NSs that are continuously emitting GWs as “GW pulsars”. By “unknown”, we mean that the GW pulsar’s position on the sky, frequency, and frequency derivatives are all unknown, and so must be searched over. (The NS could be unknown either because it is electromagnetically inactive, or because its electromagnetic emission does not reach us—e.g., because we do not intersect its radio pulsar beam.) Brady et al. [1] showed that straightforward matched-filter searches for unknown GW pulsars would be severely computationally limited; for example, searches for young, fast NSs (NSs with GW frequencies as high as 1 kHz and spin-down ages as short as 40 yr) would be limited to observation times of order one day. To address this problem, Brady & Creighton [2] (henceforth referred to as BC) were the first to consider hierarchical, multistage, semi-coherent searches for GW pulsars. Briefly, a semi-coherent search is one where a sequence of short data stretches are all coherently searched, using some technique akin to matched filtering, and then the

resulting powers from the different stretches are summed. The method is only “semi-coherent” because powers are added instead of complex amplitudes; i.e., information regarding the overall phase of the signal in different stretches is discarded. This allows one to use a much coarser grid on parameter space than would be required in a fully coherent search of the same data. BC developed a “stack-slide” method for summing the powers along different tracks in the time-frequency plane, in close analogy to the “power stacking” method (sometimes called the Radon transform) used in radio pulsar searches. The basic idea of their two-stage search is to identify a list of “candidates” (basically, promising-looking regions in parameter space) in the first stage, using some fraction of the available data, and then to “follow up” those candidates using more data in the second stage. In their scheme, both the first and second stages are semi-coherent.

In this paper we revisit the problem of constructing efficient, hierarchical searches for GW pulsars. We build on the BC treatment, but we also significantly generalize and otherwise improve upon their work. The most important improvements are that we consider searches with n semi-coherent stages (not just 2), with surviving candidates being winnowed at each stage, and we add on a fully coherent final stage to verify or debunk any remaining candidates. We also explicitly account for the unknown polarization of the source, while this complication was omitted for in BC, for simplicity. Other important differences between our work and theirs will be highlighted below.

This paper is organized as follows. Section II sets up notation, describes the expected signal from an isolated GW pulsar, and reviews the stack-slide algorithm. Our general multistage strategy for searching through large parameter spaces for GW pulsars, using a combination of semi-coherent methods and coherent methods, is ex-

^{*}Electronic address: curt.cutler@aei.mpg.de

[†]Electronic address: iraj.gholami@aei.mpg.de

[‡]Electronic address: badri.krishnan@aei.mpg.de

plained in Section III. Our general search scheme contains a fair number of free parameters (the number and duration of the coherently analyzed stretches in each semi-coherent stage, as well as the coarseness of the discrete grid used to cover the parameter space of sought-for signals), which we can adjust to make the search as efficient as possible. Our general scheme for performing this optimization is described in Section III B. Section IV develops all the formulae we need to evaluate the computational cost of any of our strategies, for any desired sensitivity. More specifically, section IV A reviews the template-counting formulae developed in BC; section IV B develops the equations relating the thresholds that candidates must pass at different stages (to advance to the following stage) to the false dismissal (FD) rates at those stages, and hence to the overall sensitivity of the search; and section IV C derives estimates for the dominant computational cost of each part of the search. Section V describes our results: the optimal strategy (within our general scheme) and its sensitivity. Section VI concludes with a summary of our main results and a discussion of open issues and future work.

II. NOTATION AND BASICS

A. The signal from a GW pulsar

Here we briefly review the expected GW signal from a spinning neutron star. Let $x(t)$ be the output of some detector. In the absence of any signal, $x(t)$ is just noise $n(t)$, which we shall assume to be a stationary, Gaussian stochastic process with zero mean. In the presence of a signal, we have

$$x(t) = n(t) + h(t) \quad (1)$$

where the signal $h(t)$ is a deterministic function of time. We assume that the GW pulsar is isolated and at rest with respect to us, so that effects due to its motion can be neglected. (More precisely, we assume these effects can be absorbed into an overall Doppler shift, and so are unobservable.) Let t_{ssb} be time measured in the Solar System Barycenter (SSB) frame. The form of $h(t)$ in this frame is a constant-amplitude sinusoid with phase given by

$$\Phi(t_{\text{ssb}}) = \Phi_0 + 2\pi f_0 \Delta t_{\text{ssb}} + 2\pi \sum_{k=1}^s \frac{f_k}{(k+1)!} (\Delta t_{\text{ssb}})^{k+1} \quad (2)$$

where $\Delta t_{\text{ssb}} \equiv t_{\text{ssb}} - t_{\text{ssb}}^{(0)}$, with $t_{\text{ssb}}^{(0)}$ being a fiducial start time; Φ_0 , f_0 and f_k are respectively the phase, frequency, and spin-down parameters at the start time, and s is the number of spin-down parameters that we search over. Assuming that the pulsar is isolated and emitting GWs due to a small deviation from axisymmetry, the waveforms

for the two polarizations are

$$h_+ = \frac{1}{2} h_0 (1 + \cos^2 \iota) \cos \Phi(t), \quad (3)$$

$$h_\times = h_0 \cos \iota \sin \Phi(t) \quad (4)$$

where h_0 represents the angle-independent amplitude of the wave, ι is the angle between the spin-axis of the pulsar and the direction of the waves' propagation, and the frequency $f = \dot{\Phi}/2\pi$ of the emitted GWs is equal to twice the rotational frequency of the star.

Let \mathbf{n} be the unit vector pointing from the Solar System toward the pulsar, $\mathbf{r}(t)$ be the position of the detector in the SSB frame, and $\mathbf{v}(t)$ be its velocity with t being the time in the detector frame. Ignoring relativistic corrections [19], a wave reaching the Sun at time t_{ssb} will reach the detector at time

$$t = t_{\text{ssb}} - \frac{\mathbf{r}(t) \cdot \mathbf{n}}{c}. \quad (5)$$

As seen from Eqs. (2) and (5), to a good approximation, the instantaneous frequency of the signal as seen by the detector is given by the familiar Doppler shift expression

$$f(t) = \hat{f}(t) \left(1 + \frac{\mathbf{v}(t) \cdot \mathbf{n}}{c} \right) \quad (6)$$

where $\hat{f}(t)$ is the instantaneous frequency of the signal in the SSB frame, and is given by

$$\hat{f}(t) = f_0 + \sum_{k=1}^s \frac{f_k}{k!} (\Delta t_{\text{ssb}})^k. \quad (7)$$

Eqs. (6) and (7) describe the frequency modulation of the received signal. The received signal is also amplitude modulated by the time-changing antenna pattern of the detector as it is carried along by the Earth's rotation. The received signal $h(t)$ is a linear combination of h_+ and h_\times :

$$h(t) = F_+(\mathbf{n}, \psi) h_+(t) + F_\times(\mathbf{n}, \psi) h_\times(t) \quad (8)$$

where ψ is the polarization angle of the signal, and $F_{+,\times}$ are the antenna pattern functions. Due to the motion of the Earth, the $F_{+,\times}$ depend implicitly on time:

$$F_+(t) = a(t) \cos 2\psi + b(t) \sin 2\psi \quad (9)$$

$$F_\times(t) = b(t) \cos 2\psi - a(t) \sin 2\psi \quad (10)$$

where the functions $a(t)$ and $b(t)$ are independent of ψ . (In these equations, the angle between the arms of the detector is taken to be $\pi/2$.) We refer the reader to [3] for explicit expressions for $a(t)$ and $b(t)$.

The modulated frequency is described by the $s+3$ parameters consisting of f_0 and $\vec{\lambda} := (\mathbf{n}, \{f_k\}_{k=1\dots s})$; we shall often denote the pair $(f_0, \vec{\lambda})$ by the boldface symbol $\boldsymbol{\lambda}$. Apart from the parameters $\boldsymbol{\lambda}$, the waveform (8) depends on other parameters: the pulsar's orientation ι ,

polarization angle ψ , the initial phase Φ_0 , and the amplitude h_0 . The optimal matched filter statistic [3] for detecting the waveform must, in principle, search over the entire parameter space $(\lambda, \iota, \psi, \Phi_0, h_0)$. However, it turns out that the computationally challenging part of the search involves just the λ ; the optimization of over $(\iota, \psi, \Phi_0, h_0)$ can be done analytically, by means of the \mathcal{F} -statistic defined in [3]. The \mathcal{F} -statistic is the optimal matched filter statistic maximized over $(\iota, \psi, \Phi_0, h_0)$. It is therefore only a function of $(f_0, \vec{\lambda})$ and it is given by

$$\mathcal{F}(f_0, \vec{\lambda}) = 4 \left[\frac{B|F_a|^2 + A|F_b|^2 - 2C\mathcal{R}(F_a F_b^*)}{\Delta T S_n(f_0) D} \right] \quad (11)$$

where $S_n(f)$ is the single-sided power spectral density of the detector noise $n(t)$, and

$$F_a = \int_{-\Delta T/2}^{\Delta T/2} x(t) a(t) e^{-i\Phi(t; \lambda)} dt, \quad (12)$$

$$F_b = \int_{-\Delta T/2}^{\Delta T/2} x(t) b(t) e^{-i\Phi(t; \lambda)} dt, \quad (13)$$

$$A = (a|a), \quad B = (b|b), \quad (14)$$

$$C = (a|b), \quad D = AB - C^2. \quad (15)$$

Here we have used the notation

$$(x|y) = \frac{2}{\Delta T} \int_{-\Delta T/2}^{\Delta T/2} x(t) y(t) dt. \quad (16)$$

In cases where the amplitude modulation can be ignored (e.g., for short data segments, $\ll 1$ day long, where the $a(t)$ and $b(t)$ can be approximated as constant), we see that \mathcal{F} is proportional to the demodulated Fourier transform which matches just the phase evolution:

$$\mathcal{F} \propto |\tilde{X}(f, \vec{\lambda})|^2 \quad (17)$$

where

$$\tilde{X}(f, \lambda) = \int_{-\Delta T/2}^{\Delta T/2} x(t) e^{-i\Phi(t; \lambda)} dt. \quad (18)$$

The \mathcal{F} -statistic is the optimal (frequentist) detection statistic for GW pulsars, and it is at the core of some algorithms currently used to search for GW pulsars in LIGO and GEO data [4]. Some important properties of the \mathcal{F} -statistic are reviewed in section IV.B, and a more detailed description can be found in [3].

B. The Stack-Slide algorithm

The stack-slide algorithm is best described with reference to the Doppler shift formula of Eq. (6). Imagine we have a data stream $x(t)$ covering an observation time T_{used} , and we wish to search for a GW pulsar with some parameters λ . We break up the data into N smaller segments of length $\Delta T = T_{\text{used}}/N$, and calculate the Fourier

spectrum of each segment. For now we assume each segment is sufficiently short that the signal frequency remains confined to a single discrete frequency bin. If there is a signal present, it will most likely be too weak to show up in a single segment with any significant signal-to-noise-ratio (SNR). However, we can increase the SNR by adding the power from the different segments. We must *not* use the the same frequency bin from each segment, but rather must follow the frequency evolution given by Eq. (6). Thus, we ‘stack’ the power after ‘sliding’ each segment in frequency space. Note that the sliding depends on $\vec{\lambda}$. Thus, in practice, we choose a grid in the space of $\vec{\lambda}$ ’s and the sliding is done differently at each grid point.

As described above, the sensitivity of the stack-slide algorithm is restricted due to the length of ΔT ; we should not take ΔT to be too large, since then we would lose SNR due to the signal power being spread over several frequency bins. However, we can gather all the signal power back into a single bin by taking account of the Doppler modulation and spin-down while calculating the spectrum of a segment; i.e., we de-modulate each data segment before summing.

With these concepts at hand, we can now describe the stack-slide search for the \mathcal{F} -statistic. The strategy is very similar to the power summing method described earlier in this section. Again we break up the data of length T_{used} into N segments, each of length $\Delta T = T_{\text{used}}/N$. We choose a point $\vec{\lambda}_d$ in parameter space, and demodulate the signal accordingly. We calculate $\mathcal{F}(f, \vec{\lambda}_d)$ as a function of the frequency for each segment and add the \mathcal{F} -statistic values after sliding the different segments in frequency space appropriately.

As explained in BC, the resolution of sky- and spin-down-space that suffices for the demodulation is not fine enough for for the stack-slide step. Thus at each stage we two grids on parameter space: a coarse one for performing the short-segment demodulations and a fine one for sliding and stacking the short-segment results. We refer the reader to [5] and the appendix of [6] for a detailed derivation of the formula relating the required amount of sliding to the parameters $\vec{\lambda}_d$.

III. A MULTISTAGE HIERARCHICAL SEARCH

A. The general algorithm

The stack-slide search algorithm described in the previous section has two components: 1) calculation of the \mathcal{F} -statistic for data stretches of length ΔT , 2) summation of the resulting \mathcal{F} values along the appropriate tracks in the time-frequency plane. (If there are N coherently analyzed segments, then the sums have N terms.) If we had unlimited computational resources, we would simply do a fully coherent search on all the data; i.e., set $N = 1$ and take ΔT to be the entire observation time. However, the

number of templates required for a fully coherent search increases as a high power of ΔT , making this impractical for all-sky searches.

To illustrate this point, consider an all-sky search for young, fast pulsars, i.e., GW pulsars that have a spin-down age as short as $\tau_{\min} = 40$ yr and that emit GWs with frequency up to $f_{\max} = 1000$ Hz. Let us assume that we have 30 days of data available to us. Imagine two different ways of looking for this pulsar: a full 30-day coherent integration versus a semi-coherent method where the available data is broken up into 30 equal segments. The formula for the number of templates required for these searches is given below in Eq (30). It turns out that the full coherent search requires $\sim 4.2 \times 10^{15}$ templates if we are to not lose more than 30% of the signal power. On the other hand, the semi-coherent search requires only $\sim 1.5 \times 10^{11}$ templates for the same allowed fractional loss in signal power. The ratio of the the number of templates required for the two types of searches increases rapidly with the observation time; for instance, for an observation time of 40 days, the corresponding numbers are $\sim 5.5 \times 10^{16}$ and $\sim 8.3 \times 10^{11}$ for the full coherent and semi-coherent searches respectively.

As illustrated by the above example, semi-coherent searches for unknown GW pulsars are a compromise forced upon us by limited computing power. Such searches will remain computationally limited for the foreseeable future, so it behooves us to organize them as efficiently as possible. In this paper we consider a class of multistage, hierarchical search algorithms. Since our main “problem” is the large volume of parameter space we need to search over, the basic idea behind these algorithms is to identify and discard unpromising regions of parameter space as fast as possible—without discarding real signals. The type of scheme we consider is illustrated schematically in Fig. 1. The first stage is a semi-coherent search through some fraction of the available data. A threshold is set, and candidates exceeding this threshold are passed to the next stage. The second stage is similar to the first, but includes additional data and generally entails a finer resolution of parameter space. (The latter means that any candidate that survives the first semi-coherent stage gives rise to a little crowd of nearby candidates that are examined in the second semi-coherent stage.) Any candidate that exceeds the second-stage threshold is passed on to the third stage, and so on. In an $(n + 1)$ -stage search, any candidate surviving all n semi-coherent selections is subjected to a final, coherent search (which we consider the $(n + 1)^{\text{th}}$ stage); if the final, coherent threshold is exceeded, then a detection is announced. We impose as a constraint that the false alarm (FA) rate for the entire search must be $< 1\%$; i.e., if the data is actually just noise, then the probability that a detection is announced must be $< 1\%$. For reasons explained below, in realistic examples this inequality is all too easy to satisfy; the actual FA rate for our optimized searches is typically smaller than 1% by many orders of magnitude.

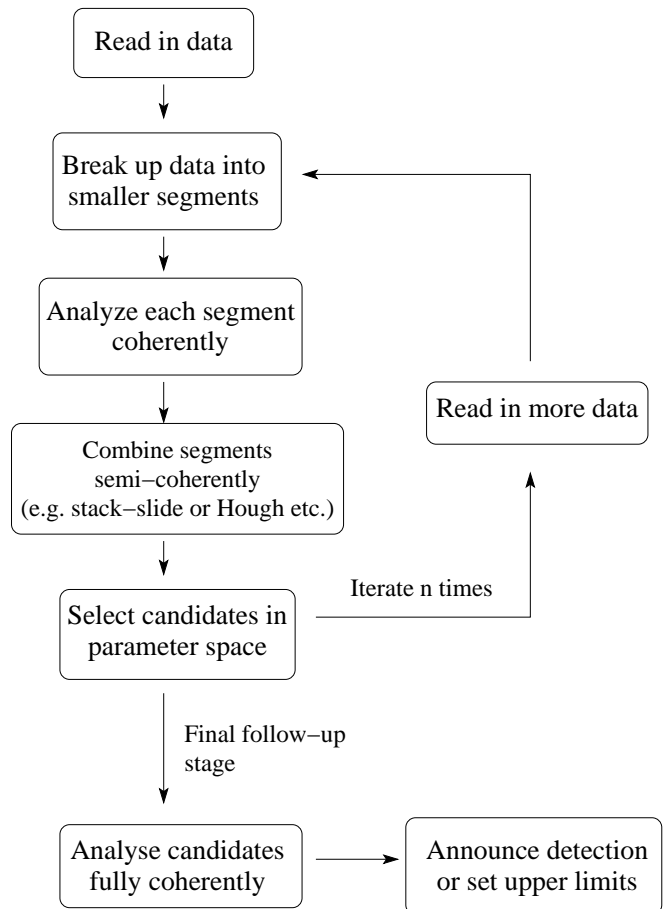


FIG. 1: A hierarchical scheme for the analysis of large parameter space volumes for continuous wave searches. Each step analyzes only those regions in parameter space that have not been discarded by any of the previous steps.

In the end, our search will be able to detect a GW pulsar signal whose rms strength (at the detector) h_{RMS} exceeds some threshold value h_{th} (with a false dismissal rate of 10 – 15%). We can think of $1/h_{\text{th}}$ as the search’s sensitivity. We will optimize our search to get the maximum sensitivity for any given computing power or, equivalently, to find the minimum computer power necessary to attain any given sensitivity.

The problem of optimizing a semi-coherent, hierarchical search scheme for GW pulsars was first studied by BC. The present study builds upon the BC formalism, but there are also some important differences. We call attention to the following ones:

- 1) BC consider a hierarchical search consisting of exactly two semi-coherent stages. In the present work, we consider a search consisting of an arbitrary number of semi-coherent steps, plus a fully coherent, “follow-up” stage (utilizing all the available data) to assess the significance of any surviving candidates. The effect of the final, follow-up stage is to ensure that the overall false alarm rate (fixed at

exactly 1% by BC) is greatly reduced and, for all practical purposes, ceases to be a constraint.

- 2) In BC's second semi-coherent stage, all the data used in the first-stage is reanalyzed, along with some "fresh" (as yet unanalyzed) data. *A priori*, it is not clear whether this strategy is more efficient than one in which each semi-coherent stage analyzes only fresh data. (E.g, the first stage analyzes 20 days of data and generates candidates, the second semi-coherent stage searches for those candidates in the *next* 50 days of data and generates a list of candidates that have still "survived", these survivors are searched for again in the *next* 150 days of data, etc.) In this paper, we investigate both kinds of schemes: schemes where previously analyzed data is always *recycled* into subsequent stages, and schemes where each semi-coherent stage analyzes only fresh data.
- 3) For simplicity, BC ignored the fact that the GWs have two possible polarizations (in effect pretending that the detectors measure a scalar wave). This is a reasonable approximation when estimating the number of grid-points needed to cover the parameter space, but not, say, when trying to estimate the FA and FD rates as a function of the threshold at some intermediate stage in the search. (Roughly speaking, scalar waves with the same matched-filter SNR would be easier to detect than actual GWs, since with GWs the full SNR is "split" between the two polarizations, in a way that is unknown *a priori*.) In this paper we aim to make realistic estimates of a GW pulsar's detectability for a given matched-filter SNR (and given region of parameter space to be searched over), so we take polarization into account wherever it makes a significant difference. In practice, this just means that we use the \mathcal{F} -statistic, Eq. (11), as our detection statistic.
- 4) When estimating computational costs, BC assume that the demodulations will be done using *stroboscopic re-sampling*, a method modeled closely on the FFT algorithm. A different demodulation method, which we shall refer to as the SFT method, is currently being used by the GW pulsar search codes in the LIGO Scientific Collaboration (LSC) software library [7]. The SFT method takes as its input a short FFT database (FFT'ed sets of short-time data stretches), and can be more efficient than *stroboscopic re-sampling* in cases where only a narrow frequency range of the demodulated time series is of interest. In this paper we explore the possibility of using different demodulation methods at different stages of the search, and attempt to find the most efficient combination.

All the above points will be elaborated on in later sections of the paper.

B. The general optimization scheme

In this section we further discuss our search algorithm and its optimization. First we establish some notation. Let n be the total number of semi-coherent stages. Let $N^{(i)}$ be the number of stacks used in the i^{th} stage and $\Delta T^{(i)}$ be the length of each stack; the superscript i will always refer to the i^{th} semi-coherent stage. The resolution of the template grid used to cover parameter space is given in terms of the maximum fractional mismatch in signal power $\mu_{\text{max}}^{(i)}$ [8]. Our detection statistic is $\rho^{(i)}$, the sum of the \mathcal{F} values from the different stacks (obtained after sliding appropriately):

$$\rho^{(i)} = \sum_{k=1}^{N^{(i)}} \mathcal{F}_k^{(i)}. \quad (19)$$

Denote the distribution of $\rho^{(i)}$ in the absence of any signal by $p(\rho^{(i)})$. In the presence of a GW signal of amplitude h_{RMS} , let the distribution of $\rho^{(i)}$ at the gridpoint nearest the actual signal be $p(\rho^{(i)}|h_{\text{RMS}}, \mu_{\text{max}}^{(i)})$. Let $\rho_{\text{th}}^{(i)}$ be the i^{th} -stage threshold, which a candidate must exceed to advance to the next stage. that we use to reject candidates or advance them to the next stage. The i^{th} -stage FA rate (per candidate) $\alpha^{(i)}$ and FD rate (per candidate) $\beta^{(i)}$ are given by

$$\alpha^{(i)}(\rho_{\text{th}}^{(i)}) = \int_{\rho_{\text{th}}^{(i)}}^{\infty} p(\rho) d\rho, \quad (20)$$

$$\beta^{(i)}(\rho_{\text{th}}^{(i)}; h_{\text{RMS}}, \mu_{\text{max}}^{(i)}) = \int_0^{\rho_{\text{th}}^{(i)}} p(\rho|h_{\text{RMS}}, \mu_{\text{max}}^{(i)}) d\rho. \quad (21)$$

Practically identical formulae apply to the final, coherent stage as well.

Again, we require of any search algorithm that, at the very end of the search, it results in a false detection less than 1% of the time. Given this constraint, we parametrize the search's sensitivity by the signal amplitude h_{th} such that an embedded signal with $h_{\text{RMS}} > h_{\text{th}}$ would be detected $\gtrsim 85 - 90\%$ of the time. We enforce the latter condition as follows. We set the first-stage threshold h_{th} such that a signal of amplitude $h_{\text{RMS}} = h_{\text{th}}$ will pass to the second stage 90% of the time. At all subsequent stages we set the threshold such that the same signal with strength $h_{\text{RMS}} = h_{\text{th}}$ has a 99% chance of passing to the next higher stage. That is, we adjust the the i^{th} -stage threshold $\rho_{\text{th}}^{(i)}$ so that $\beta^{(1)} = 0.10$, while $\beta^{(i)} = 0.01$ for $i > 1$, and $\beta^{(\text{coh})} = 0.01$ as well. The motivation behind making $\beta^{(1)}$ lower than $\beta^{(i)}$ for $i > 1$ is the following: We believe that a computationally efficient algorithm will have the property that a true signal that is strong enough to pass the first-stage threshold *should* generally pass over all the others. Any source that is not sufficiently strong to make it through to the end of the detection pipeline should be discarded as soon as possible, so as not to waste computing power. This reflects

the basic idea behind our hierarchical searches: to eliminate unpromising regions of parameter space as quickly as possible, so that computational resources can be focused on the more promising regions. Basically, the first-stage threshold determines the sensitivity of the whole search, and subsequent steps whittle down the number of candidates (i.e., the number of small patches in parameter space that perhaps contain a true signal) until any remaining patches can be fully, coherently analyzed.

To fully specify our search algorithm, we have to choose the parameters $\Gamma \equiv (n, \{N^{(i)}\}, \{\Delta T^{(i)}\}, \{\mu_{\max}^{(i)}\}, \mu_{\max}^{coh})$, where n is the number of semi-coherent stages and $i = 1, \dots, n$. In doing so, we are subject to certain requirements or constraints:

- The total amount of data available is no more than some T_{\max} (say, 1 year).
- We wish to detect (with $\sim 90\%$ FD rate and $< 1\%$ overall FA rate) any unknown signal of amplitude h_{RMS} greater than h_{th} (say, 10^{-26}).

Our task is to choose the parameters Γ that minimize the total required computational power P , subject to the above constraints. We arrive at a cost function $P(h_{th})$, the computational cost of reaching any given sensitivity level. (Really, P is function of the product $h_{th}^2 T_{\max}/S_n(f)$, but we are regarding T_{\max} and $S_n(f)$ as fixed.) We can immediately invert this function to determine $h_{th}(P)$, the sensitivity achievable for any given computing power.

Let us first deal with the constraint on the total amount of data. We are going to consider simultaneously two different modes of all-sky searches. In “data recycling mode,” at each stage we start back at the beginning of the data, but take progressively larger values of $N^{(i)}\Delta T^{(i)}$. Thus the first stage looks at data in the interval $[T_0, T_0 + N^{(1)}\Delta T^{(1)}]$, the second stage looks at $[T_0, T_0 + N^{(2)}\Delta T^{(2)}]$ and so on. The total observation time is thus

$$T_{\text{used}} = N^{(n)}\Delta T^{(n)}. \quad (22)$$

In “fresh-data” mode, rather than always starting over from the beginning, we analyze fresh data at each stage. The first stage looks at data in the range $[T_0, T_0 + N^{(1)}\Delta T^{(1)}]$, the second stage looks at $[T_0 + N^{(1)}\Delta T^{(1)}, T_0 + N^{(1)}\Delta T^{(1)} + N^{(2)}\Delta T^{(2)}]$, etc. The total observation time is thus

$$T_{\text{used}} = \sum_{i=1}^n N^{(i)}\Delta T^{(i)}. \quad (23)$$

In either data-recycling or fresh-data mode, one constraint is that $T_{\text{used}} \leq T_{\max}$ where T_{\max} is the total amount of data available. Also, in either mode, at each stage we look only at portions of parameter space that exceeded the threshold set at the previous stage.

Next we consider our constraints on the overall FA and FD rates for the pipeline. The final, coherent follow-up

stage is expected to be much more sensitive than any of the preceding steps; therefore the overall FA rate is essentially set by the final stage threshold alone. (The earlier stages serve only to whittle down the number of candidates, N_{coh} , that are analyzed in the final coherent stage.) If the threshold in the final follow-up stage is $\rho_{th}^{(coh)}$, then the overall FA rate is no larger than $\alpha^{(coh)}(\rho_{th}^{(coh)})$ times the number of effectively independent candidates in parameter space. We approximate the latter, crudely, by $\sim N_p(T_{\max}, 0.2, 1)$; in practice $\alpha^{(coh)}(\rho_{th}^{(coh)})$ turns out to be so minuscule that the crudeness of this approximation is irrelevant.

The overall false dismissal requirement is also easily handled. Let $\tilde{\beta}$ be the total false dismissal rate of the multistage search. Each stage has its own threshold $\rho_{th}^{(i)}$ and corresponding false dismissal rate $\beta^{(i)}$. If each stage, including the follow-up stage, were to analyze completely independent data, we would have

$$\tilde{\beta} = 1 - \prod_{i=1}^{n+1} (1 - \beta^{(i)}) \approx \beta^{(1)} + \dots + \beta^{(n+1)}. \quad (24)$$

(where we use “ $\beta^{(n+1)}$ ” interchangeably with $\beta^{(coh)}$). In our fresh-data search mode, the data at different stages are independent, *except* for the final, follow-up stage. And in our recycled-data scheme, the data examined at higher stages includes all the data examined in earlier stages. Then when $\beta^{(1)} = 0.1$ and

$$\beta^{(2)} = \beta^{(3)} = \dots = \beta^{(n)} = \beta^{(coh)} = 0.01, \quad (25)$$

it is clear that $\tilde{\beta}$ is roughly in the range $(10 + n - 1)\%$ to $(10 + n)\%$, *for fresh-data mode and 10% to $(10 + n)\%$ for recycled-data mode*. Since $n \approx 3$ turns out to be optimal (see below), we crudely summarize this by saying that our strategies have an overall FD rate of 10 – 15% at the threshold value of h_{RMS} .

Finally, we turn to the search’s computational cost, which we wish to minimize. Let us denote the total number of floating point operations for the i^{th} semi-coherent stage by $C^{(i)}$ and for the final coherent stage by $C^{(coh)}$. Expressions for $C^{(i)}$ and $C^{(coh)}$ are given in the next section. For now, it is sufficient to say the total computational cost is

$$C_{\text{total}} = \left(\sum_{i=1}^n C^{(i)} \right) + C^{(coh)}, \quad (26)$$

and that if we wish to analyze the data in roughly real time, the required computational power (operations per unit time) is

$$P = \frac{C_{\text{total}}}{T_{\text{used}}}. \quad (27)$$

Depending on which mode we are working in, T_{used} is given by Eq. (22) or Eq. (23).

Again, our strategy for optimizing the search is to minimize P , subject to the constraints listed above.

IV. TEMPLATE COUNTING, CONFIDENCE LEVELS, AND COMPUTATIONAL COST

A. Template counting formulae

This section gives the template counting formulae originally derived by BC using the metric formulation developed in [8].

For simplicity, the parameter space is covered by spheres of proper radius $\sqrt{\mu_{\max}}$ (μ_{\max} is the maximum allowed fractional mismatch in the detection statistic [8]) using a cubic grid. However it is worth keeping in mind that a cubic grid over-estimates the number of required templates even in two dimensions, and the difference increases rapidly with the dimensionality [9].

As mentioned earlier, for each semi-coherent stage, we have a coarse grid for the demodulation and a fine grid for the stack-slide analysis. Following BC, for simplicity we shall require that at any given semi-coherent stage, the maximal mismatch μ_{\max} for the fine grid is the same as μ_{\max} for the coarse one. However (unlike BC), we allow μ_{\max} to vary from one stage to the next.

The number of templates (or gridpoints) N_p is a function of the mismatch μ_{\max} , the coherent time baseline ΔT , and the number of stacks N (which is unity for the coarse grid). BC have derived the following expressions for the number of gridpoints, N_{pc} and N_{pf} , in the coarse and fine grids, respectively:

$$N_{pc} = N_p(\Delta T, \mu_{\max}, 1), \quad (28)$$

$$N_{pf} = N_p(\Delta T, \mu_{\max}, N). \quad (29)$$

where N_p is given in Eq. (2.22) of BC:

$$N_p = \max_{s \in \{0,1,2,3\}} \left[\mathcal{M}_s \mathcal{N}_s G_s \prod_{k=0}^s \left(1 + \frac{0.3r\Omega^{k+1}\tau_{\min}^k}{c k! \sqrt{\mathcal{M}_s}} \right) \right]. \quad (30)$$

Here $r = 1$ AU is Earth's orbital radius, $\Omega = 2\pi/(1\text{yr})$,

$$\mathcal{N}_s = \frac{s^{s/2}}{(s+2)^{s/2}} \frac{f_{\max}^s \Delta T^{s(s+3)/2}}{(\mu_{\max}/s)^{s/2} \tau_{\min}^{s(s+1)/2}}, \quad (31)$$

$$\mathcal{M}_s = \left(\frac{f_{\max}}{1\text{Hz}} \right)^2 \frac{(s+2)}{4\mu_{\max}} \left(\frac{1}{A^2} + \frac{1}{B^2} + \frac{1}{C^2} \right)^{-1/2}, \quad (32)$$

where

$$A = 0.014, B = 0.046 \left(\frac{\Delta T}{1 \text{ day}} \right)^2, C = 0.18 \left(\frac{\Delta T}{1 \text{ day}} \right)^5 \quad (33)$$

and the functions G_s are given in Appendix A of BC. Roughly speaking, the factor \mathcal{M}_s counts distinct patches on the sky as set by the Earth's one-day spin period, \mathcal{N}_s counts distinct "patches" in the space of spin-down parameters, the G_s give the dependence of N_p on the number of stacks, N , and the factors of the form

$\left(1 + \frac{0.3r\Omega^{k+1}\tau_{\min}^k}{c k! \sqrt{\mathcal{M}_s}} \right)$ effectively account for the increase of search volume required when the frequency derivative $d^k f/dt^k$ is dominated by the Doppler shift from the Earth's motion around the Sun rather than by the pulsar's intrinsic spin-down. In our numerical work we use the full expressions for the G_s given in the Appendix A of BC, but for completeness we note that BC also give the following approximate fits to the G_s , which are valid when $N \gg 4$:

$$G_0(N) = 1, \quad (34)$$

$$G_1(N) \approx 0.524N, \quad (35)$$

$$G_2(N) \approx 0.0708N^3, \quad (36)$$

$$G_3(N) \approx 0.00243N^6. \quad (37)$$

The N_p results in BC were derived under the assumption that the observation time is significantly less than one year. As we shall see below, in the cases where the total available data covers an observation time of a year or more, it turns out that for the optimal search, the initial semi-coherent stages typically analyze a few days' to a few months' worth of data. Also, most of the search's computational cost is spent on these early stages. (This is especially true for the young-pulsar search, which is the most computationally challenging.) Therefore, it seems reasonable for our purposes to simply use the N_p formulae from BC for *all* observation times. Since the cost-errors we make by using the BS formulae will be confined to the later stages, and since the overall sensitivity of the search is effectively set at the first stage, we believe these errors will not significantly affect the total computational cost, for fixed threshold (though they may affect the relative allocation of resources between the different stage). Of course, the validity of this assumption can only really be checked by re-doing the calculation using more accurate expressions for the N_p 's, appropriate for year-long observation times, but unfortunately such expressions are not currently available.

Even for short observation times, the N_p calculation in BC used the approximation (17), which neglects the amplitude modulation of the signal; however this approximation is not expected to cause significant errors in estimating template numbers.

B. False dismissal rates and the thresholds

In this subsection, we discuss the statistical properties of the stack-slide search and solve the false dismissal constraint to obtain expressions for the thresholds.

It is shown in [3] that the distribution of the \mathcal{F} -statistic (or to be more precise, $2\mathcal{F}$), for each coherent search, is given by a non-central χ^2 distribution. The non-centrality parameter η is given in terms of the signal $h(t)$

by:

$$\begin{aligned}\eta &= 4 \left(1 - \frac{\mu_{\max}}{3}\right) \int_0^\infty \frac{|\tilde{h}(f)|^2}{S_n(f)} df \\ &= \left(1 - \frac{\mu_{\max}}{3}\right) \frac{2h_{\text{RMS}}^2 \Delta T}{S_n(f)},\end{aligned}\quad (38)$$

where $\tilde{h}(f)$ is the Fourier transform of $h(t)$. We have included a fitting factor of $1 - \mu_{\max}/3$ to account for the average loss in power due to the mismatch between the signal and template. h_{RMS} is the root-mean-square value of the signal $h(t)$. We can relate h_{RMS} to the amplitude h_{RMS} defined in Eqs. (3) and (4), as follows. If one averages h_{RMS} over all sky-positions as well as over the polarization parameters ι and ψ , one obtains $\langle h_{\text{RMS}}^2 \rangle = (2/25)h_0^2$ (see Eq. (93) of [3]).

More explicitly, the distribution is

$$\begin{aligned}p(\mathcal{F}|\eta) &= 2\chi^2(2\mathcal{F}|\eta, 4) \\ &= \left(\frac{2\mathcal{F}}{\eta}\right)^{1/2} I_1(\sqrt{2\mathcal{F}\eta}) e^{-\mathcal{F}-\eta/2}\end{aligned}\quad (39)$$

where $\chi^2(\cdot|\eta, \nu)$ is the χ^2 distribution with ν degrees of freedom and non-centrality parameter η , and I_1 is the modified Bessel function of first order. The statistic ρ of interest for the stack-slide search is the sum of the \mathcal{F} -statistic over N stacks. Assuming the \mathcal{F} -statistic for the N stacks to be statistically independent, 2ρ must follow a χ^2 distribution with $4N$ degrees of freedom and non-centrality parameter $N\eta$

$$p(\rho|\eta, N) = 2\chi^2(2\rho|N\eta, 4N). \quad (40)$$

The mean and variance of ρ are given respectively by

$$\bar{\rho} = 2N + \frac{N\eta}{2}, \quad \sigma_\rho^2 = 2N + N\eta. \quad (41)$$

Using the distribution $p(\rho^{(i)})$, the false alarm rate for the i^{th} semi-coherent stage (defined in Eq. (20)) can be evaluated analytically:

$$\alpha^{(i)}(\rho_{\text{th}}^{(i)}) = e^{-\rho_{\text{th}}^{(i)}} \sum_{k=0}^{2N^{(i)}-1} \frac{(\rho_{\text{th}}^{(i)})^k}{k!}. \quad (42)$$

As discussed earlier, the overall false alarm probability $\tilde{\alpha}$ for the search is set by the final coherent follow-up stage. For this stage, $N = 1$ so that if the threshold on ρ is $\rho_{\text{th}}^{(\text{coh})}$, then it is easy to see from the previous equation that:

$$\tilde{\alpha} = (1 + \rho_{\text{th}}^{(\text{coh})}) e^{-\rho_{\text{th}}^{(\text{coh})}}. \quad (43)$$

In the presence of a signal, the non-central χ^2 distribution for ρ is a little cumbersome to work with, and it is useful to replace it by a Gaussian with the appropriate mean and variance. So we say that the distribution of ρ must

be approximately Gaussian with mean and variance as in eq. (41):

$$p(\rho|\eta, N) = \frac{1}{\sqrt{2\pi\sigma_\rho^2}} e^{-(\rho-\bar{\rho})^2/2\sigma_\rho^2}. \quad (44)$$

This approximation is not valid when N is of order unity. Then for any given h_{th} , we should set the threshold of the i^{th} stage, $\rho^{(i)}$ by the false dismissal requirement:

$$\int_0^{\rho^{(i)}} p(\rho|\eta_{\text{th}}^{(i)}, N) d\rho = \beta^{(i)}, \quad (45)$$

where

$$\eta_{\text{th}}^{(i)} := \left(1 - \frac{\mu_{\max}}{3}\right) \frac{2h_{\text{th}}^2 \Delta T^{(i)}}{S_n(f)}. \quad (46)$$

Here the factor of $1 - \mu_{\max}^{(i)}/3$ accounts for the average loss in power due to the mismatch between the signal parameters and nearest gridpoint parameters. Eq. (45) can be solved to find $\rho_{\text{th}}^{(i)}$ as a function of h_{th} , $\Delta T^{(i)}$, and $\mu^{(i)}$. Or equivalently, it gives $h_{\text{th}} = h_{\text{th}}(\rho^{(i)}, \Delta T^{(i)}, \mu^{(i)})$. This equation can easily be solved by using the properties of the complementary error function. By changing variables in the integral, we can rewrite the false dismissal rate as

$$\beta^{(i)} = \frac{1}{2} \text{erfc}\left(\frac{\bar{\rho}^{(i)} - \rho^{(i)}}{\sqrt{2}\sigma_\rho^{(i)}}\right). \quad (47)$$

If h_{th} is the smallest value of h_{RMS} for which the false dismissal rate is no bigger than $\beta^{(i)}$, then we have

$$\begin{aligned}\rho^{(i)}(h_{\text{th}}) &= \bar{\rho}^{(i)} - \sqrt{2}\sigma_\rho^{(i)} \text{erfc}^{-1}(2\beta^{(i)}) \\ &\approx 2N^{(i)} \left[1 + \frac{\eta_{\text{th}}^{(i)}}{4}\right] \\ &\quad - 2\text{erfc}^{-1}(2\beta^{(i)}) \sqrt{N^{(i)}} \sqrt{1 + \frac{\eta_{\text{th}}^{(i)}}{2}}.\end{aligned}\quad (48)$$

In practice, we fix one value of h_{th} (our sensitivity goal) for an entire search, and we then set the threshold $\rho^{(i)}$ at each stage by solving Eq. (48), with the false dismissal rates set by $\beta^{(1)} = 0.1$ and $\beta^{(i)} = \beta^{\text{coh}} = 0.01$ for $i \geq 2$. Our rationale for this choice is as follows. At each stage, one can estimate the signal strength of any successful candidate. If after the first stage, one can already predict that a candidate is not strong enough to pass over the threshold at the second or a higher stage, then one might as well discard it immediately and so not waste computer power on a likely failure. Put the other way, an efficient algorithm should ensure that a true signal that is strong enough to pass over the first stage is also strong enough to pass over all subsequent stages. Then the false dismissal rate for the whole search will be only a little larger than the FD rate of the first stage alone, or a little more than 10%. (An *overestimate* of the total FD rate is the sum of the rates for each of the stages, or 13% for a 3-stage search.)

C. Computational Cost

Let us begin with the first semi-coherent stage. Here, the number of points in the coarse and fine grids are respectively

$$N_{pc}^{(1)} = N_p(\Delta T^{(1)}, \mu_{\max}^{(1)}, 1), \quad (49)$$

$$N_{pf}^{(1)} = N_p(\Delta T^{(1)}, \mu_{\max}^{(1)}, N^{(1)}). \quad (50)$$

If we are searching in a frequency range from small frequencies up to f_{\max} , the data must be sampled in the time domain (at least) at the Nyquist frequency $2f_{\max}$. The minimum number of data points that we must start out with in the time domain is then $2f_{\max}\Delta T$. To calculate the \mathcal{F} -statistic for each stack, we need to first calculate the quantities F_a and F_b which appear in equation (11). We describe two methods below which may be called the *stroboscopic resampling method* and the *SFT method*. Given F_a and F_b , the cost of combining them to get \mathcal{F} is negligible.

The stroboscopic resampling method: The method suggested in [3] (and also in [2]) is based on the observation that the integrals in Eqs. (12) and (13) look *almost* like a Fourier transform; the difference being the form of $\Phi(t)$ in the exponential. However, by suitably resampling the time series, effectively redefining the time variable so that the spectrum of a real signal would look like a spike in a single frequency bin, the integral can be written as a Fourier transform and we can then use the FFT algorithm. Since the cost of calculating an FFT for a time series containing m data points is $3m \log_2 m$, the operations cost of calculating the \mathcal{F} -statistic for each stack should be approximately $12f_{\max}\Delta T \log_2(2f_{\max}\Delta T)$. Repeating this for $N^{(1)}$ stacks and for each point in the coarse grid, we see that the total cost of calculating F_a and F_b , and therefore the \mathcal{F} -statistic, is approximately

$$12N^{(1)}N_{pc}^{(1)}f_{\max}\Delta T^{(1)}\log_2(2f_{\max}\Delta T^{(1)}). \quad (51)$$

We now need to appropriately slide each segment in frequency space and stack them up, i.e. add the \mathcal{F} -statistic values from each stack to get our final statistic ρ . This has to be done for each point in the fine grid. The cost of sliding is negligible and we need only consider the cost of adding the \mathcal{F} -statistic values. Since adding $N^{(1)}$ real numbers requires $N^{(1)} - 1$ floating point operations, we see that the cost of stacking and sliding for all frequency bins and for all points in the fine grid is approximately

$$f_{\max}\Delta T^{(1)}N_{pf}^{(1)}(N^{(1)} - 1). \quad (52)$$

Thus, the computational cost for the first semi-coherent stage is

$$C_{\text{res}}^{(1)} = f_{\max}\Delta T^{(1)}N_{pc}^{(1)}\left[12N^{(1)}\frac{\log(2f_{\max}\Delta T^{(1)})}{\log 2} + \frac{N_{pf}^{(1)}}{N_{pc}^{(1)}}(N^{(1)} - 1)\right]. \quad (53)$$

The subscript _{res} indicates that this result is for the stroboscopic resampling method.

The SFT method: An alternative method is to use as input not the time series, but rather a bank of short time baseline Fourier Transforms (SFTs). This is in fact the method currently being used in the search codes of the LIGO Scientific Collaboration [7]. Here one first breaks up the data into short segments of length T_{sft} , and calculates the Fourier transform of each segment. (These segments, which are to be combined *coherently*, are not to be confused with the segments used in the stack-slide algorithm which are combined incoherently). T_{sft} should be short enough so that the signal does not drift by more than half a frequency bin over this time. Typical values of T_{sft} are 1800s. The exact method of calculating the \mathcal{F} -statistic from an SFT database is sketched in Appendix A, and the operations count is also derived there. The result is (see Eq. (A12)):

$$\approx 640N^{(1)}N_{pc}^{(1)}f_{\max}\frac{(\Delta T^{(1)})^2}{T_{\text{sft}}}\text{Flops}. \quad (54)$$

Note that the SFT method of calculating the \mathcal{F} -statistic is $\mathcal{O}((\Delta T^{(1)})^2)$ while for the stroboscopic resampling method it is $\mathcal{O}(\Delta T^{(1)} \log \Delta T^{(1)})$.

The total cost of stacking and sliding in the first hierarchical stage using the SFT method is thus:

$$C_{\text{sft}}^{(1)} = f_{\max}\Delta T^{(1)}N_{pc}^{(1)}\left[\frac{640N^{(1)}\Delta T^{(1)}}{T_{\text{sft}}} + \frac{N_{pf}^{(1)}}{N_{pc}^{(1)}}(N^{(1)} - 1)\right]. \quad (55)$$

When all frequencies are to be searched over, stroboscopic resampling produces the \mathcal{F} -statistic about an order of magnitude more cheaply than the SFT method, for typical values of $\Delta T^{(1)}$. However when previous stages have narrowed the search to a small fraction of the whole frequency band (for any given $\vec{\lambda}$), the SFT method can be the more efficient one. We should also mention here that it is possible to start with SFTs and combine them in such a way as to get a $\mathcal{O}(\Delta T^{(1)} \log \Delta T^{(1)})$ operations count; this is in fact the method used in [10]. However, in this paper, by the ‘‘SFT method’’ we always mean the method described here in Appendix B, with the operation count given above in Eq. (55).

It also seems likely that the resampling method could be modified so as to be the most efficient one, even when only wanted to demodulate a small frequency band

$$\Delta f = \max\left\{1, \frac{\Delta T^{(i)}}{\Delta T^{(i-1)}}\right\} \quad (56)$$

around every selected candidate. Presumably the first step would be to heterodyne the data to shift the relevant frequency range to a neighborhood of zero-frequency. Then one would filter out frequencies higher than Δf ,

followed by the usual demodulation. Eq. (60) would then be modified, so that the new cost of demodulating would be $12N^{(i)}\Delta T^{(i)}\Delta f \log_2(2\Delta T^{(i)}\Delta f)$. However since the details of this modified demodulation method have not yet been worked out, we will not consider it further in this paper.

This completes our analysis of the first stage computational costs for both methods. The analysis for the subsequent stages proceeds similarly; the only difference is that subsequent stages analyze only those regions of parameter space that have not been discarded by any of the previous stages. Assuming that almost all the candidates are due to noise, the false alarm rate is a good estimate of the number of candidates produced by any stage. Let us denote by $F^{(i)}$ the number of candidates which survive the i^{th} stage. Since the false alarm rate for the first stage is $\alpha^{(1)}$, the number of candidates produced by the first stage is given by

$$F^{(1)} = \max \left\{ 1, f_{\max} \Delta T^{(1)} N_{pf}^{(1)} \alpha^{(1)} \right\}. \quad (57)$$

Note that we will always have at least one candidate which makes it through to the next stage. To calculate the cost of a search, we of course must make some assumptions about the data to be processed. Basically, we are assuming that the data consists of Gaussian noise plus one detectable source. (Though we call $F^{(i)}$ the “ i^{th} -stage false alarm rate”, it is really the “false alarm rate or the true-source survival rate, whichever dominates”. In practice, until the last semi-coherent stage, the FA rate always dominates.)

To estimate the computational cost for the i^{th} stage, for $i > 1$, recall that each of the $F^{(i-1)}$ candidates produced by the $(i-1)^{\text{th}}$ stage is in fact a region in parameter space. If we assume that the i^{th} stage further refines this region, then we see that the number of i^{th} -stage coarse grid points in this region must be, on average, $N_{pc}^{(i)}/N_{pf}^{(i-1)}$ (again, assuming this ratio to be bigger than 1). Thus, using the stroboscopic resampling method, the number of floating point operations to calculate the \mathcal{F} -statistic in the i^{th} stage is

$$F^{(i-1)} \max \left\{ 1, \frac{N_{pc}^{(i)}}{N_{pf}^{(i-1)}} \right\} 12f_{\max} \Delta T^{(i)} N^{(i)} \log_2(2f_{\max} \Delta T^{(i)}). \quad (58)$$

Each candidate produced by the $(i-1)^{\text{th}}$ stage occupies a frequency band $1/\Delta T^{(i-1)}$, and thus corresponds to $\Delta T^{(i)}/\Delta T^{(i-1)}$ i^{th} -stage frequency bins. Thus the operations count for the stacking and sliding is

$$F^{(i-1)} \max \left\{ 1, \frac{\Delta T^{(i)}}{\Delta T^{(i-1)}} \right\} \max \left\{ 1, \frac{N_{pc}^{(i)}}{N_{pf}^{(i-1)}} \right\} \times \frac{N_{pf}^{(i)}}{N_{pc}^{(i)}} (N^{(i)} - 1) \quad (59)$$

floating point operations. Combining these results, we

get the computational cost for the i^{th} stage ($i \geq 2$):

$$C_{\text{res}}^{(i)} = F^{(i-1)} \max \left\{ 1, \frac{N_{pc}^{(i)}}{N_{pf}^{(i-1)}} \right\} \times \left[12N^{(i)} f_{\max} \Delta T^{(i)} \frac{\log(2f_{\max} \Delta T^{(i)})}{\log 2} + \max \left\{ 1, \frac{\Delta T^{(i)}}{\Delta T^{(i-1)}} \right\} \frac{N_{pf}^{(i)}}{N_{pc}^{(i)}} (N^{(i)} - 1) \right]. \quad (60)$$

If instead one uses the SFT method for calculating the \mathcal{F} -statistic, it is easy to see the operations count is

$$C_{\text{sft}}^{(i)} = F^{(i-1)} \max \left\{ 1, \frac{N_{pc}^{(i)}}{N_{pf}^{(i-1)}} \right\} \max \left\{ 1, \frac{\Delta T^{(i)}}{\Delta T^{(i-1)}} \right\} \times \left[\frac{640N^{(i)} \Delta T^{(i)}}{T_{\text{sft}}} + \frac{N_{pf}^{(i)}}{N_{pc}^{(i)}} (N^{(i)} - 1) \right]. \quad (61)$$

After the n semi-coherent steps, we have the final coherent follow-up stage where the entire stretch of data of duration T_{used} is used. For this stage, we analyze $F^{(n)}$ candidates and simply compute the \mathcal{F} -statistic without breaking up the data into any smaller stacks. The cost $C_{\text{res}}^{(coh)}$ for this using the resampling method is

$$C_{\text{res}}^{(coh)} = F^{(n)} \max \left\{ 1, \frac{N_p^{(coh)}}{N_{pf}^{(n)}} \right\} 12f_{\max} T_{\text{used}} \frac{\log(2f_{\max} T_{\text{used}})}{\log 2} \quad (62)$$

where $N_{pf}^{(coh)} \equiv N_p(T_{\text{used}}, \mu_{coh}, 1)$, and μ_{coh} is the μ_{max} of the final, coherent stage. Using the SFT method, we would have

$$C_{\text{sft}}^{(coh)} = F^{(n)} \max \left\{ 1, \frac{N_p^{(coh)}}{N_{pf}^{(n)}} \right\} \max \left\{ 1, \frac{T_{\text{used}}}{\Delta T^{(n)}} \right\} \frac{640T_{\text{used}}}{T_{\text{sft}}} \quad (63)$$

So far, all results in this section are valid whether we are working in fresh-data mode or data-recycling mode. The following formulae, for the number of candidates which survive a given stage, do however depend on which mode we are working in. If we operate in fresh-data mode (analyzing fresh data at every stage—except the last stage, which is a coherent follow-up of all the searched data), we clearly have (for $i \geq 2$)

$$F^{(i)} = \alpha^{(i)} \max \left\{ F^{(i-1)}, 1 \right\} \max \left(1, \frac{N_{pf}^{(i)}}{N_{pc}^{(i-1)}} \right) \times \max \left(1, \frac{\Delta T^{(i)}}{\Delta T^{(i-1)}} \right). \quad (64)$$

Again, our count assumes that at least one candidate gets “promoted” to the succeeding stage. We note that Eq. (64) assumes that the parameter space resolution improves at every stage of fresh-data mode (which seems always to be true for our optimized searches). We also

note that Eq. (64) is basically identical to Eq. (5.2) of BC, but there it is claimed to be the FA rate for data-recycling mode. That is not correct, in general, as we discuss further below.

If we are in data-recycling mode (at each step, re-analyzing old data, while also adding on new data), then the probabilities of a candidate's randomly surviving the $(i-1)^{th}$ and i^{th} stages are *not* independent, and so Eq. (64) is no longer valid. (To see this, consider the limit where only a very tiny bit of data is added on, and the resolution is kept fixed. Then any candidate that survives the $(i-1)^{th}$ stage has almost a 100% chance of surviving the i^{th} stage, even if $\alpha^{(i)}$ is extremely small.) Indeed, the rhs of Eq. (64) is clearly a *lower bound* on the i^{th} -stage false alarm rate, in data-recycling mode.

We can also place the following *upper bound* on $F^{(i)}$ for data-recycling mode:

$$F^{(i)} = f_{\max} \Delta T^{(i)} N_{pf}^{(i)} \alpha^{(i)}. \quad (65)$$

The rhs of (65) is the number of false alarms that would result if one performed a semi-coherent search of the *entire* parameter space with the given $(N^{(i)}, \Delta T^{(i)}, \mu^{(i)}, \rho^{(i)})$, while the lhs is the false alarms that result from searching only neighborhoods of the points that survived the $(i-1)^{th}$ stage. Thus for data-recycling mode, we can say that $F^{(i)}$ is somewhere in the range

$$F^{(i-1)} \left(\frac{N_{pf}^{(i)}}{N_{pf}^{(i-1)}} \frac{\Delta T^{(i)}}{\Delta T^{(i-1)}} \right) \alpha^{(i)} \leq F^{(i)} \leq f_{\max} \Delta T^{(i)} N_{pf}^{(i)} \alpha^{(i)}. \quad (66)$$

Fortunately, when we calculate the total computational cost of some optimized search in data-recycling mode, needed to achieve some given sensitivity h_{th} , if we try plugging in *either* the upper or lower bound for $F^{(i)}$, we find the two final results differ from each other by $\lesssim 18\%$ for a young pulsar ($\tau_{min} = 40$ year) and $\lesssim 5\%$ for an old one ($\tau_{min} = 10^6$ year), which for our purposes is practically insignificant. Moreover, the optimized search parameters obtained when we plug in the upper-limit estimate for $F^{(i)}$ are quite similar to those we find by plugging in the lower limit instead. Therefore it is safe for us to choose *either* the upper or lower limit as an estimate of $F^{(i)}$. For concreteness, in the rest of this paper we always estimate $F^{(i)}$ by its upper limit, which slightly overestimates the computational cost of the search.

With these results in hand, we are now ready to calculate the total computational cost of the entire search pipeline. We have a number of choices to make. At each stage, we can use either the stroboscopic resampling method or the SFT method in each stage, and we can work in either the data-recycling mode or fresh-data mode from the second stage onwards. For convenience, we somewhat arbitrarily limit the choices by considering only strategies that use either data-recycling mode in every stage or fresh-data mode in every stage. As we shall

see below, the efficiencies of these two sorts of searches turn out to be extremely close anyway. Therefore we strongly suspect that more general searches (using fresh-data mode in some stages and data-recycling mode in others) would not give significant improvements.

V. RESULTS

A. The optimization method

We next describe our numerical optimization method. The function we want to minimize, the computational power of Eq. (27), is a complicated function on a large-dimensional space. Our chosen method is a simulated annealing algorithm [11, 12] based on the downhill simplex method of Nelder and Mead [13]. The downhill simplex method consists of evaluating the function on the vertices of a simplex and moving the simplex downhill and shrinking it until the desired accuracy is reached. The motion of the simplex consists of a prescribed set of “moves” which could be either an expansion of the simplex, a reflection around a face, or a contraction. This method is turned into a simulated annealing method by adding a random fluctuation to the values of the function to be minimized, at the points of the simplex. The temperature of the random fluctuations is reduced appropriately, or in other words “annealed”, until the minimum is found.

There are no universal choices for the rate of annealing or the starting point of the simplex; these depend on the particular problem at hand. For the results presented below, we have used a variety of different starting points and annealing schedules to convince ourselves that the optimization algorithm has converged and that we have indeed found the best minimum. Let us first discuss the starting temperature, whose meaning is as follows. If f is the the function to be minimized, then the temperature Θ parametrizes the amplitude of random fluctuations $f \rightarrow f + \delta f$ added to f at the points of the simplex:

$$\delta f = -\Theta \log r \quad (67)$$

where $0 < r < 1$ is a uniformly distributed random number. A simplex move is always accepted if it takes the simplex downhill, but an uphill step may also be accepted due to these random fluctuations. In our case, we found that a starting temperature of $\Theta \sim 10^6$ - 10^9 gives good convergence; this value is to be compared to the typical value $\sim 10^{13}$ of the computational cost near its minimum for most of the results presented below. We allow a maximum of 500 iterations of the simplex. If the simplex does not converge within 500 iterations, we reduce the temperature by 2 – 5% and restart the iterations from the best minimum found up to that point. These steps are repeated until the simplex converges. The starting point of the simplex cannot be chosen arbitrarily, and for this purpose, it is useful to have a rough idea of the location of the minimum. This requires some experimenting with

a sufficiently broad range of starting points; this is especially important when the number of variables is large, as is the case for, say, a search with $n > 3$. Having found a suitable starting point for one set of pulsar parameters (f_{\max} and τ_{\min}), it can be reused for nearby pulsar parameter values. Occasionally, to obtain convergence to a minimum, we have taken as our starting point the minimum we found for nearby pulsar-parameter values.

We next describe how we impose the constraint that the total amount of analyzed data is less than T_{\max} . One could imagine trying to do this using the method of Lagrange multipliers. However this seemed difficult to implement numerically (for our highly non-linear function P), and we found a simpler approach that suffices. The function our algorithm minimizes is not the total computational power P (defined in Eq. (27)) itself, but rather

$$f = P \times \left[1 + S \left(\frac{T_{\text{used}}}{T_{\text{max}}} \right) \right] \quad (68)$$

where $S(x)$ is a smooth function such that $S(x) = 0$ for $0 < x < 1$ but $S(x)$ is rapidly increasing exponential function for $x > 1$. That is, we impose a very steep penalty for leaving the constraint surface. This works well, and indeed we found it useful to impose some additional (intuitively obvious) constraints in this way, such as requiring the $N^{(i)}$ and $\Delta T^{(i)}$ to all be positive; we again multiply P by factor that is unity when the constraint is satisfied but is very large when the constraint is violated. This “trick” is used to find the *location* of the minimum, but of course the results we report are the values of the function P there, not f .

There is one additional technical detail, namely, that our optimization method is meant for the case of continuous, real variables, while our variables $N^{(i)}$ are strictly integers. We handle this by rounding off $N^{(i)}$ to the nearest integer while calculating the cost function f , every time it is called. The downhill simplex algorithm still treats $N^{(i)}$ as a continuous variable, i.e. we allow arbitrarily small changes to $N^{(i)}$ when the simplex is moving downhill, but such changes have no effect on f . We have also tried an alternative approach where $N^{(i)}$ is kept as a continuous variable throughout, and rounded off only at the very end. We have found that the two approaches yield consistent results.

Finally, we cross-checked our results using two different implementations of the simulated annealing algorithm—those of [14] and [15]—and found that they gave basically equivalent results in our case.

B. The number of semi-coherent stages

The first question we want to answer is: what is the optimum number n of semi-coherent stages to use in the search? Relatedly, we want to know the most efficient method to use for the \mathcal{F} -statistic calculation (stroboscopic resampling or SFT method) and best mode to work in (fresh-data mode or data-recycling mode). To

answer this, we consider an all-sky search for fast/young GW pulsars, by which we mean a search that goes up to frequency $f_{\max} = 1000$ Hz and that can detect pulsars with spindown ages τ_{\min} as short as 40 yr. We assume the amount of data available is $T_{\max} = 1$ yr, and ask what is the computational power required to detect pulsar signals whose h_{RMS} is or above h_{th} , given by:

$$\frac{h_{th}^2}{S_n(f)} = 2.5 \times 10^{-5} \text{sec}^{-1}. \quad (69)$$

This signal strength corresponds to $\sqrt{\eta} \approx 39.72$ for a full 1-yr observation time with a perfectly matched template. (Here and below we are implicitly assuming that $S_n(f)$ hardly varies over the frequency range of the signal.) We choose the i^{th} -stage FD rates $\beta^{(i)}$ as given in (and just above) Eq. (25), which, along with the detection threshold given by Eq. (69), determines the i^{th} -stage thresholds $\rho^{(i)}$. For simplicity, we set $\mu^{(coh)} = 0.2$. While this is a restriction that we simply put in by hand (to slightly reduce the space of search parameters to be optimized), we believe this choice has very little effect on the overall optimized strategy because, as we shall see shortly, the follow-up stage usually accounts for only a tiny fraction of the total computational cost.[20] Thus we are left with $3n$ parameters to be optimized: $(\Delta T^{(i)}, \mu_{\max}^{(i)}, N^{(i)})$ for $i = 1, \dots, n$, subject to the constraint that the total amount of data analyzed, T_{used} [given by Eq. (22) or (23)] is less than 1 yr.

Plots of the minimum computational cost for different n and for both the data-recycling and fresh-data modes are shown in Fig. 2. For each mode, we consider the following three strategies: (i) Use the SFT method in each stage, (ii) Use the resampling method in each stage, and (iii) Use the resampling method in the first and final follow-up stages, and use the SFT method in all intermediate stages. Therefore there are 6 curves in Fig. 2.

The most important lessons from Fig. 2 are the following: Strategy (iii) turns out to be better than (i) or (ii). Furthermore, for strategy (iii), there is a significant advantage in a three-stage search as compared to a two-stage or single-stage search, but there is hardly any improvement in computational cost in going to four or more semi-coherent stages. Furthermore, these results are the same whether we use the fresh-data mode or data-recycling mode, and these two modes give very similar total costs. While Fig. 2 presents results just for young/fast pulsar searches, we find the same basic pattern for old pulsars, with $\tau_{\min} \sim 10^6$ yr: strategy (ii) is the most efficient for calculating the \mathcal{F} -statistic, data-recycling mode and fresh-data mode are almost equally efficient, and having three semi-coherent stages is near-optimal (significantly better than two stages, and practically as good as four). The main difference from the young/fast pulsar case is that the gain in going from 2 to 3 stages is now only a factor ~ 2 in computational power, i.e., smaller but still significant.

In the light of these results, in the rest of this section, we consider only three-stage searches, with the first

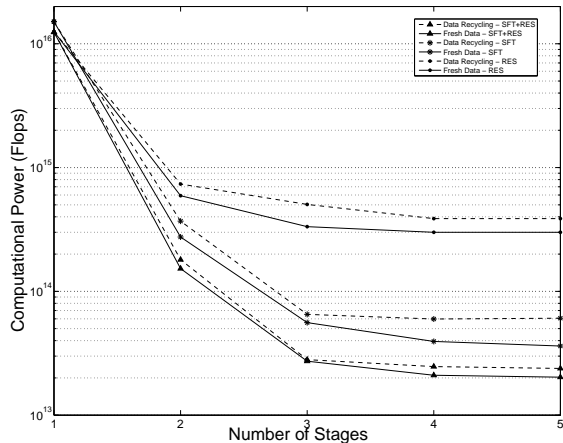


FIG. 2: Computational power versus number of semi-coherent stages for different methods of calculating the \mathcal{F} -statistic. RES indicates the stroboscopic resampling method (strategy (ii)) and SFT is the SFT method (strategy (i)). SFT+RES corresponds the mixture of these two methods (strategy (iii)). For each strategy, solid lines indicate the result for the fresh-data mode, while the dashed lines are for the data-recycling mode.

stage and final follow-up stages employing the resampling method and with the second and third stages employing the SFT method. We continue to report results for both data-recycling mode and fresh-data mode.

C. The optimal three-stage search parameters

For the example search described above, (i.e. $f_{\max} = 1000$ Hz, $\tau_{\min} = 40$ yr, $T_{\max} = 1$ yr, and $h_{th}^2/S_n = 2.5 \times 10^{-5} \text{sec}^{-1}$) we list the optimal search parameters for the three-stage search in data-recycling mode in Table I. The first two stages analyze about 26 days (divided in 10 segments) and 42 days (divided in 12 segments) of data, respectively, while the third stage analyzes the entire year-long data stretch (divided in 8 segments). The total computational cost is 40.2 TFlops. The cost breakdown among the individual stages, and further cost breakdown into the demodulation piece $C_{coh}^{(i)}$ and the stack-slide $C_{ss}^{(i)}$ piece in each stage, are given in Table II. There we give the total count of floating point operations required, not the number of operations per second.

Our results for fresh-data mode are qualitatively similar, and are given in Table III. In this case, the optimal search analyzes about 24 days of data in the first stage (broken up into 9 segments) and 24 more days in the second stage (broken into 6 segments). The third stage analyzes the rest of the year’s worth of data, divided into 7 segments. The total computational requirement is 34.6 TFlops and its breakdown is given in Table IV.

TABLE I: The optimal search parameters in data recycling mode. $f_{\max} = 1000$ Hz, $\tau_{\min} = 40$ yr, $T_{\max} = 1$ yr, $h_{th}^2/S_n = 2.5 \times 10^{-5} \text{sec}^{-1}$, and η is defined according to Eq. 38.

Stage	$\Delta T^{(i)}$ (days)	$\mu^{(i)}$	$N^{(i)}$	$T_{\text{used}}^{(i)}$ (days)	$\sqrt{\eta}$
1	2.58	0.7805	10	25.79	9.08
2	3.51	0.1139	12	42.13	13.23
3	45.66	0.8196	8	365.25	33.86

TABLE II: The computational cost to analyze one year of data in data-recycling mode. The search parameters are the same as given in Table I. $C_{coh}^{(i)}$ is the cost for the coherent demodulation step and $C_{ss}^{(i)}$ for the stack-slide step, while $C^{(i)}$ is the sum of these two. Follow-up indicates the computational cost require for the final follow-up stage.

Stage	$C^{(i)}$ (Flop)	$C_{coh}^{(i)}$ (Flop)	$C_{ss}^{(i)}$ (Flop)
1	9.37×10^{20}	6.21×10^{19}	8.75×10^{20}
2	3.16×10^{20}	2.46×10^{20}	6.98×10^{19}
3	1.65×10^{19}	2.73×10^{18}	1.37×10^{19}
Follow-up	6.30×10^{15}		

We note the following features of these results. First, in both modes, basically all the data has been analyzed by the end of the third semi-coherent stage. This is not a requirement that we put in by hand, but rather it arises from the optimization: the optimal scheme “gets through” the entire year’s worth of data before the final follow-up stage. Secondly, in data-recycling mode, 73.8% of the computing time is spent in the first stage, 24.9% in the second, 1.3% in the third and a negligible fraction in the follow-up. The results are similar for the fresh-data mode: approximately 74.2% of the computational resources are spent in the first stage, 24.2% in the second stage, 1.6% in the third stage and a negligible amount in the follow up stage. Finally, fresh-data mode entails a slightly lower computational cost than data-recycling mode. However this last fact could be an artifact either of having slightly different overall FD rates in the two cases, or of our using an overestimate of $F^{(i)}$ in the lat-

TABLE III: Same as Table I, but for fresh-data mode.

Stage	$\Delta T^{(i)}$ (days)	$\mu^{(i)}$	$N^{(i)}$	$T_{\text{used}}^{(i)}$ (days)	$\sqrt{\eta}$
1	2.71	0.7829	9	24.35	8.82
2	4.08	0.0654	6	24.49	10.17
3	45.20	0.8229	7	316.42	31.50

TABLE IV: Same as Table II, but for fresh-data mode.

Stage	$C^{(i)}$ (Flop)	$C_{\text{coh}}^{(i)}$ (Flop)	$C_{ss}^{(i)}$ (Flop)
1	8.11×10^{20}	6.42×10^{19}	7.46×10^{20}
2	2.64×10^{20}	2.62×10^{20}	2.67×10^{18}
3	1.74×10^{19}	5.54×10^{18}	1.19×10^{19}
Follow-up	1.62×10^{16}		

TABLE V: Search parameters for data-recycling mode with $f_{\text{max}} = 1000\text{Hz}$, $\tau_{\text{min}} = 10^6\text{yr}$, $T_{\text{max}} = 1\text{yr}$, $h_{th}^2/S_n = 4.53 \times 10^{-6}\text{sec}^{-1}$, and computational power 40.2Tflops; η is defined according to Eq. (38).

Stage	$\Delta T^{(i)}$ (days)	$\mu^{(i)}$	$N^{(i)}$	$T_{\text{used}}^{(i)}$ (days)	$\sqrt{\eta}$
1	14.84	0.3514	8	118.72	9.06
2	30.06	0.0917	6	180.34	11.70
3	52.18	0.0986	7	365.25	16.63

ter case. The bottom line is that, after optimization, the two modes are almost equally efficient.

If instead we consider a search for older pulsars, with $\tau_{\text{min}} = 10^6\text{yr}$ instead of 40 yr, then the optimal solution for both modes are summarized in Tables V–VIII. A larger value of τ_{min} means a smaller number of templates, and therefore a more sensitive search for fixed computational cost.

For data-recycling mode, we have lowered the threshold h_{th} by a factor 2.35, to the point where the required computational power is again 40.2 Tflops, as in the example of Tables I and II. The results are shown in tables V and VI. Compared to the young-pulsar search, the computational power is now spread more evenly over the first two stages: the first stage consumes about 58.27% of the power, the second stage 38.73%, third stage 3.0% and negligible for the follow-up stage.

For the case of fresh-data mode, we have lowered the threshold h_{th} by a factor 2.36, to the point where the required computational power is again 34.6 Tflops, as in the example of Tables III and IV. Once again, compared to the young-pulsar search, the computational costs are spread more evenly over the first two stages: the first stage consumes about 31.3% of the power, the second stage 30.4%, third stage 14.0%. In this case, the cost for the follow-up stage is 24.0%, which is not negligible. This indicates that, for this case, the earlier stages have not succeeded in reducing the number of candidates to a low level. The overall sensitivity, though, is still almost identical to the data-recycling case.

Let us now discuss the false alarm rate. We require that the overall FA rate be less than 1%, and we claimed in section III B that this is automatically satisfied in typi-

TABLE VI: The computational cost to analyze one year of data in data-recycling mode. The search parameters are the same as given in Table V. $C_{\text{coh}}^{(i)}$ is the cost for the coherent demodulation step and $C_{ss}^{(i)}$ for the stack-slide step, while $C^{(i)}$ is the sum of these two. Follow-up indicates the computational cost require for the final follow-up stage.

Stage	$C^{(i)}$ (Flop)	$C_{\text{coh}}^{(i)}$ (Flop)	$C_{ss}^{(i)}$ (Flop)
1	7.41×10^{20}	2.85×10^{18}	7.39×10^{20}
2	4.93×10^{20}	3.77×10^{20}	1.16×10^{20}
3	3.82×10^{19}	1.34×10^{19}	2.48×10^{19}
Follow-up	6.18×10^{13}		

TABLE VII: Search parameters for fresh-data mode with $f_{\text{max}} = 1000\text{Hz}$, $\tau_{\text{min}} = 10^6\text{yr}$, $T_{\text{max}} = 1\text{yr}$, $h_{th}^2/S_n = 4.47 \times 10^{-6}\text{sec}^{-1}$, and computational power 34.6Tflops; η is defined according to Eq. 38.

Stage	$\Delta T^{(i)}$ (days)	$\mu^{(i)}$	$N^{(i)}$	$T_{\text{used}}^{(i)}$ (days)	$\sqrt{\eta}$
1	11.77	0.2074	9	105.96	9.04
2	10.97	0.0199	6	65.82	7.13
3	27.64	0.0206	7	193.47	12.22

cal, realistic cases. We can now verify this claim. For the $\tau_{\text{min}} = 40\text{yr}$ search summarized in tables I–IV, using (38), with $\mu_{\text{max}} = \mu_{\text{max}}^{(\text{coh})} = 0.2$, the threshold corresponds to $\rho_{\text{th}}^{(\text{coh})} \approx \bar{\rho} = 2 + \eta/2 \approx 738$. By Eq. (43), this corresponds to $\tilde{\alpha} \approx 10^{-318}$ (for either mode). Using Eq. (30), the number of independent templates required for a full coherent search of the entire parameter space, using 1 yr of data, is $f_{\text{max}}T_{\text{max}}N_p(1\text{yr}, 0.2, 1) \approx 10^{34}$. The overall false alarm rate is thus $FA = f_{\text{max}}T_{\text{max}}N_p\tilde{\alpha} \approx 10^{-284} \ll 1\%$ [21].

Similarly, for the case $\tau_{\text{min}} = 10^6\text{yr}$, $h_{th}^2/S_n = 4.53 \times 10^{-6}$ (data recycling mode, tables V and VI), we get $\eta \approx 286$ so that $\tilde{\alpha} \approx 10^{-61}$. In this case, have $N_p \approx 10^{17}$ so that $FA = f_{\text{max}}T_{\text{max}}N_p\tilde{\alpha} \approx 10^{-34}$. If we look at

TABLE VIII: Same as Table VI, except for fresh-data mode. The search parameters are those of Table VII.

Stage	$C^{(i)}$ (Flop)	$C_{\text{coh}}^{(i)}$ (Flop)	$C_{ss}^{(i)}$ (Flop)
1	3.46×10^{20}	3.07×10^{18}	3.43×10^{20}
2	3.35×10^{20}	3.33×10^{20}	1.91×10^{18}
3	1.54×10^{20}	9.23×10^{19}	6.19×10^{19}
Follow-up	2.67×10^{20}		

fresh data mode (tables VII and VIII) with $\tau_{\min} = 10^6$ yr, $h_{th}^2/S_n = 4.47 \times 10^{-6}$, we get $FA \approx 10^{-33}$. These values are greater than for the case of young pulsars, but still vastly smaller than 1%.

The basic point is simply this: For an all-sky search, sensitivity is limited by computing power, so the detection threshold h_{th} in practice is substantially higher than what it would be for infinite computing power. This means that for a signal to be detectable, it must have quite a high SNR (in the matched filter sense)—which means that the FA rate is exponentially small. Being computationally limited means that when we *do* detect something, we can be very confident that it is not simply random noise masquerading as a signal [22]

How accurate are our numerical results? The total computational cost is a complicated function on a 9-dimensional space and thus is not easy to visualize. We can, however, take appropriate sections of this function to examine its behavior near the minimum. Thus, we can ask whether variations in, say, $\Delta T^{(1)}$ or $\Delta T^{(2)}$ away from their optimal values, increase the computational cost (as they should, if should if we have truly found a minimum). To answer this, in Fig. 3 we plot the total computational power as a function of $\Delta T^{(1)}$ and $\Delta T^{(2)}$, respectively, for the young-pulsar searches summarized in Tables I-IV. All the other parameters fixed at their optimal values. The minima of these curves agree precisely with our simulated annealing results. Similarly, Figs. 4 and 5 carry the same message, as well as showing the strong dependence of the computational cost on $N^{(i)}$ and $\mu_{\max}^{(i)}$. (It is not so clear from the plot of P vs. $\mu_{\max}^{(3)}$ that this curve has a minimum in the range shown, but it does in fact have a very shallow one.)

For the plot of computational cost versus $N^{(3)}$, we are not allowed to keep $\Delta T^{(3)}$ fixed, since that could violate the constraint $\Delta T^{(3)}N^{(3)} \leq T_{\max}$. (Recall that $\Delta T^{(3)}N^{(3)} = T_{\max} = 1$ yr for the optimal 3-stage solution, which is therefore just at the boundary of the constraint region.) Therefore, we choose to plot the computational cost as a function of $N^{(3)}$ while simultaneously varying $\Delta T^{(3)}$ according to $\Delta T^{(3)} = T_{\max}/N^{(3)}$.

A noteworthy feature of these plots is that the computational power P depends more sensitively on the early-stage parameters than the late-stage ones; e.g., more sensitively on $N^{(1)}$ and $N^{(2)}$ than on $N^{(3)}$. This result should not be surprising since, as mentioned earlier, for the young-pulsar search the computational cost of the higher stages is relatively small.

D. The spindown-age and the SNR

How does the (minimum) computational cost depend on the shortest spindown timescale that we search over, τ_{\min} ? Consider again the case where we have one year of data and we perform an all-sky search up to a frequency of $f_{\max} = 1000$ Hz. Fig. 6 shows the result for the both data-recycling and fresh-data mode, for two different val-

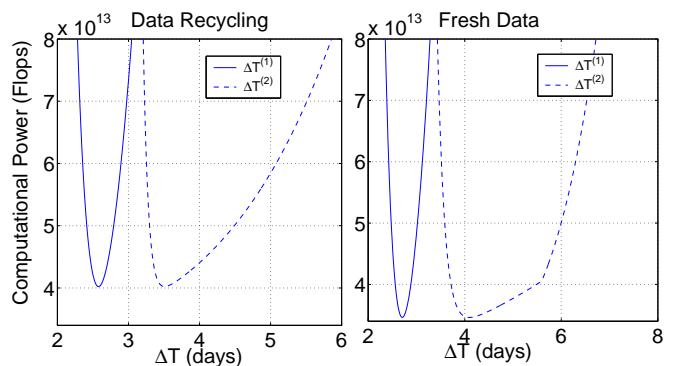


FIG. 3: Computational power P as a function of $\Delta T^{(1)}$ and $\Delta T^{(2)}$, with all other parameters fixed to their optimal values.

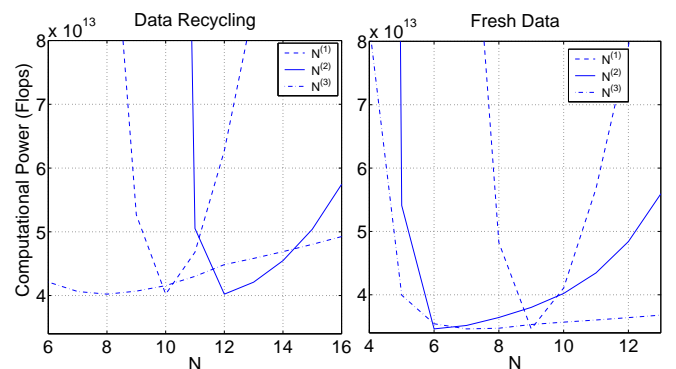


FIG. 4: Computational power P as a function of $N^{(1)}$, $N^{(2)}$ and $N^{(3)}$. For the $N^{(1)}$ and $N^{(2)}$ plots, all other parameters have fixed to their optimal values. For the $N^{(3)}$ plot, we have also varied $\Delta T^{(3)}$ according to $\Delta T^{(3)} = T_{\max}/N^{(3)}$ in order to satisfy the constraint that the amount of data available is T_{\max} .

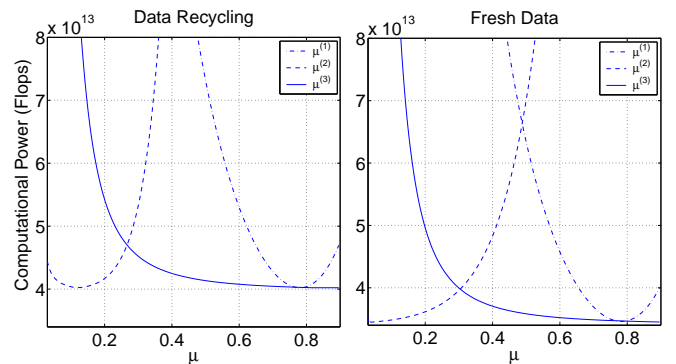


FIG. 5: Computational power P as a function of $\mu_{\max}^{(1)}$, $\mu_{\max}^{(2)}$, and $\mu_{\max}^{(3)}$. For each plot, all other parameters are fixed at their optimal values.

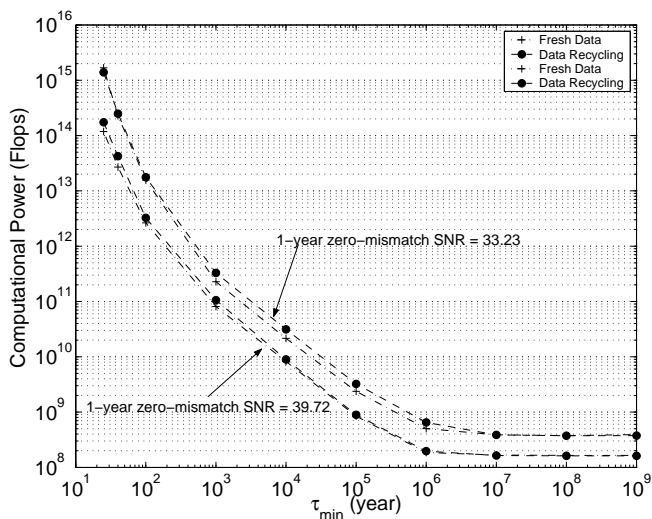


FIG. 6: The minimum computational power P required for analyzing 1 year’s worth of data as a function of the pulsar’s spindown age τ_{\min} . We consider a three-stage search in the both data-recycling and fresh-data mode, for two different signal strengths. The data-recycling mode results are shown with dashed lines, while the fresh-data results are in dotted lines. In parts of the curves, the results for the two modes are so close together that it is hard to distinguish them.

ues of the 1-year SNR. Note that these results do pass simple sanity checks: the computational cost decreases as the SNR increases (since it is easier to look for stronger signals), and the computational cost decreases as τ_{\min} increases (since it is easier to search through a smaller parameter space).

One can also ask: for a given available computational power, how does the threshold SNR scale with τ_{\min} ? This is shown in Fig. 7. The plot is based on the assumption that we have one year’s worth of data and that we have 10 TFlops of computing power at our disposal. By “SNR”, here we mean the matched-filter SNR, for a perfectly matched filter. Fig. 7 tells us that a search for unknown GW pulsars with spindown ages $> 10^6$ yr can detect $\sim 85 - 90\%$ of pulsars whose SNR is > 17 (again, with FA rate $\ll 1\%$). In an all-sky search for very young pulsars, with $\tau_{\min} = 40$ yr, the SNR required for detection (with the same FD and FA rates) increases to ~ 43 . In comparison, for a source where the sky position and frequency are known in advance (from radio observations), an SNR of only 4.56 is required for detection, with a 10% FD rate and 1% FA rate [4].

Fig. 7 strongly suggests that one would like to simultaneously perform at least two different all-sky searches: one for old GW pulsars and another for young ones, with comparable (within a factor ten) computer power devoted to each, but with quite different thresholds. (If one set the same threshold for both old and young pulsars, then almost all computing resources would end up being spent on the young ones.) Clearly, to deter-

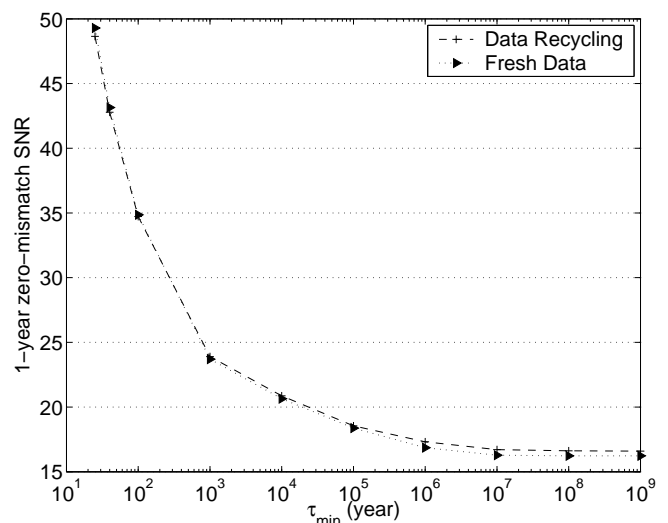


FIG. 7: The 1-year SNR (with zero mismatch) as a function of τ_{\min} , for fixed computational power $P = 10^{13}$ Flops. The dashed line indicates the result for data-recycling mode and the dotted line for fresh-data. Since these two result are very close to each other, it may be difficult to distinguish them.

mine the “best” apportionment of resources between the two types of searches would require some additional inputs/assumptions, but at least Fig. 7 seems a good first step towards making an intelligent allocation.

VI. CONCLUSIONS

Let us first summarize the main results of this paper. We have studied general hierarchical strategies for searching for gravitational waves from unknown, isolated GW pulsars. In particular, we have considered multistage hierarchical algorithms where each stage (except the last) consists of a coherent demodulation of short stacks of data followed by appropriate sliding and stacking of the \mathcal{F} -statistics results from the different stacks. The successive stages serve to quickly reduce the number of candidates; they are followed by final coherent follow-up stage to fully analyze the remaining candidates.

We have optimized this strategy by minimizing the computational cost P subject to the constraints which specify the total amount of data available and the desired confidence levels. Of course, P depends on the size of the parameter space— in particular on the range of frequencies and spindown ages that are searched over. Carrying out the optimization, and varying over the number n of semi-coherent stages, we found that the advantages of the multistage approach saturate at $n = 3$ (i.e., $n = 4$ and 5 are scarcely better).

The optimized search parameters ($N^{(i)}, \Delta T^{(i)}, \mu^{(i)}$) we report should only be considered a rough guide for carrying out a search in practice because i) in many places we

have used theoretical estimates of the operations counts instead of those obtained by profiling existing codes, ii) we have not considered issues of memory storage or the cost of performing any Monte-Carlo simulations, and iii) the detector noise has throughout been assumed to be Gaussian and stationary. Furthermore, the template counting formulae (30) used in this paper are, strictly speaking, valid only for observation times significantly less than a year. The numbers presented in this work must be recalculated when better approximations become available. In spite of these limitations, we believe that our results do provide a useful qualitative guide to what an optimized all-sky search “looks like.” In order to optimize actual search codes, applied to actual data, one must 1) profile the codes to determine the actual computational cost of the different operations, and 2) do Monte Carlo studies to determine the *actual* $\alpha^{(i)}$ for different thresholds. (Recall that the formulae given here are based on the assumption stationary, Gaussian noise.) The latter could require considerable work, especially if the results are strongly frequency-dependent, with some bands being much “better behaved” than others.

Finally, we mention some other possibilities for future work:

- It would be trivial to extend our work to consider searches that are less computationally challenging than all-sky ones, but that are still computationally limited. E.g., one could consider searches for unknown NSs in supernova remnants (such as SN 1987A), in which case the sky-position is well known but the frequency and spindown parameters must be searched over. Similarly, one could consider a search over a small fraction of sky, e.g., a portion containing the Galactic center or the disk.
- The formulae for operations counts, confidence levels etc. can also be derived for case when the Hough transform [6] is used in the semi-coherent stages instead of the stack-slide method; the optimization of multistage, hierarchical Hough-type searches would then proceed in the same way as developed here.
- We expect that the lessons learned in this paper will carry over to searches for GW pulsars in low-mass X-ray binaries, which are also a computationally limited [16]. However the details are yet to be worked out.
- The problem of searching, in LISA data, for the inspiral signals of stellar-mass compact objects captured by $\sim 10^6 M_\odot$ BHs in galactic nuclei, is similar to the GW pulsar search problem, but even more computationally challenging [18]. We expect that the lessons learned in this paper will also be very useful in formulating and optimizing a search algorithm for LISA capture sources.
- In this paper we have tacitly assumed that the search is performed by a single computer or computing cluster. However, at least in the next

few years, the most computationally intensive GW searches will be directed by **Einstein@Home**[17], which relies on tens of thousands of individual participants donating their idle computing power. In this case, there might be additional constraints that we have not yet considered, relating to the rate at which data and intermediate results can be sent back and forth between the **Einstein@Home**[17] servers and participants’ computers, how much storage is available for use on participants’ computers, etc. We intend to study hierarchical searches in this context also, to see which if any of the lessons learned here must be modified for the **Einstein@Home** context.

Acknowledgements

The authors thank Bruce Allen, Teviet Creighton, Maria Alessandra Papa, Reinhard Prix, Bernard Schutz, Xavier Siemens and Alicia Sintes for valuable discussions. BK acknowledges the hospitality of the University of the Balearic Islands in Spain.

APPENDIX A: COMPUTATIONAL COST OF THE SFT METHOD

Here we estimate the computational cost (in floating point operations) of calculating the \mathcal{F} -statistic via the SFT method. This result is used in Sec.IV.C.

We begin by reviewing the details of the SFT method; our description closely follows that given in the documentation of the software package LIGO Algorithms Library [7]. Imagine that we wish to compute the \mathcal{F} -statistic for a data stretch of length ΔT . Divide this data into M shorter segments of length $T_{\text{sft}} = \Delta T/M$, each containing N data points (so there are MN data points within ΔT). The sampled values of $x(t)$ can then be written as $x_{\alpha j}$ where $0 \leq \alpha < M$ labels the segment and $0 \leq j < N$ labels points within a segment. Eq. (12) can then be discretized as follows:

$$F_a(\boldsymbol{\lambda}) = \sum_{\alpha=0}^{M-1} \sum_{j=0}^{N-1} a_{\alpha j} x_{\alpha j} e^{-i\Phi_{\alpha j}(\boldsymbol{\lambda})} \quad (\text{A1})$$

and similarly for Eq. (13). Let $\tilde{x}_{\alpha k}$ be the discrete Fourier transform of $x_{\alpha j}$ along the index j , so that

$$x_{\alpha j} = \frac{1}{N} \sum_{k=0}^{N-1} \tilde{x}_{\alpha k} e^{2\pi i j k / N}. \quad (\text{A2})$$

Then if we approximate the amplitude modulation function $a(t)$ as constant over the short-time baseline T_{sft} , the

expression for F_a becomes

$$F_a(\boldsymbol{\lambda}) = \sum_{\alpha=0}^{M-1} a_\alpha \sum_{k=0}^{N-1} \tilde{x}_{\alpha k} \left[\frac{1}{N} \sum_{j=0}^{N-1} \exp\left(\frac{2\pi i j k}{N} - i\Phi_{\alpha j}(\boldsymbol{\lambda})\right) \right] \quad (\text{A3})$$

The short-time baseline T_{sft} is generally chosen so that neither pulsar spindown nor the Doppler effect causes the signal power to shift by more than, say, half a frequency bin. Then we can find functions $A_\alpha(\vec{\lambda})$ and $B_{\alpha k}(\boldsymbol{\lambda})$ such that to a good approximation

$$\Phi_{\alpha j}(\vec{\lambda}) - \frac{2\pi j k}{N} = A_\alpha(\vec{\lambda}) + \frac{B_{\alpha k}(\boldsymbol{\lambda})j}{N}. \quad (\text{A4})$$

Thus we have

$$\begin{aligned} & \frac{1}{N} \sum_{j=0}^{N-1} \exp\left(\frac{2\pi i j k}{N} - i\Phi_{\alpha j}(\boldsymbol{\lambda})\right) \\ &= e^{-iA_\alpha(\vec{\lambda})} \left(\frac{1 - e^{-iB_{\alpha k}(\boldsymbol{\lambda})}}{1 - e^{-iB_{\alpha k}(\boldsymbol{\lambda})/N}} \right). \end{aligned} \quad (\text{A5})$$

Next we assume N is large enough that $1 - e^{-iB_{\alpha k}(\boldsymbol{\lambda})/N} \approx iB_{\alpha k}(\boldsymbol{\lambda})/N$; then

$$F_a = \sum_{\alpha=0}^{M-1} a_\alpha e^{-iA_\alpha(\vec{\lambda})} \sum_{k=0}^{N-1} \tilde{x}_{\alpha k} P[B_{\alpha k}(\boldsymbol{\lambda})] \quad (\text{A6})$$

where

$$\begin{aligned} P[x] &= \frac{1}{N} \frac{1 - e^{-ix}}{1 - e^{-ix/N}} \\ &\approx \frac{\sin x}{x} - i \frac{1 - \cos x}{x}. \end{aligned} \quad (\text{A7})$$

Now arises the great advantage of the SFT method: the function $P[x]$ is sharply peaked about $x = 0$, so the sum over k can be approximated by retaining only a few terms:

$$F_a = \sum_{\alpha=0}^{M-1} a_\alpha e^{-iA_\alpha(\vec{\lambda})} \sum_{k'=-D}^D \tilde{x}_{\alpha k'} P[B_{\alpha k'}(\boldsymbol{\lambda})] \quad (\text{A8})$$

where $k' = k - k^*$ and k^* is the value of k such that $B_{\alpha k^*}(\boldsymbol{\lambda}) = 0$, and D is the number of terms that we retain in the sum on either side of k^* . It turns out that $D = 16$ suffices to calculate the \mathcal{F} -statistic to within a few percent.

Eq. (A8) is our final approximation for F_a . Analogous expressions hold for F_b , and the final \mathcal{F} -statistic is calculated from F_a and F_b using Eq. (11). Thus, with the SFT

method, for each point λ in parameter space we need to calculate $A_\alpha(\vec{\lambda})$, $B_{\alpha k}(\boldsymbol{\lambda})$, and the amplitude modulation functions, a_α and b_α , and then to perform the sums in Eq. (A8). It is then easy to see that to calculate the \mathcal{F} -statistic for n frequency bins, for a fixed value of $\vec{\lambda}$, the number of floating point operations required is roughly some constant times nMD . To estimate the constant, let C_1 be the cost of calculating $P[B_{\alpha k}]$ for each α and k value. Since multiplying two complex numbers requires 6 operations, and adding two complex numbers requires 2 operations, we see that calculating the sum over k' in equation (A8) requires

$$(C_1 + 6)(2D + 1) + 4D \quad (\text{A9})$$

operations. Similarly, if C_2 is the cost of calculating $a_\alpha e^{-iA_\alpha}$ for every α , then the cost of calculating F_a is

$$M[(C_1 + 6)(2D + 1) + 4D] + MC_2 + 6M + 2(M - 1). \quad (\text{A10})$$

Thus, to find F_a and F_b for every frequency bin requires $\approx 2 \times (2C_1 + 16)DM$ operations. Since the cost of combining F_a and F_b to get \mathcal{F} is negligible compared to this, and assuming C_1 to be of order unity, we see that the operation count for calculating the \mathcal{F} -statistic for n frequency bins is approximately

$$\sim 40nMD. \quad (\text{A11})$$

For the first stage in the hierarchical search, the \mathcal{F} -statistic is evaluated for $N^{(1)}N_{pc}^{(1)}f_{\text{max}}\Delta T$ bins. So, taking $D = 16$ and using $M = \Delta T^{(1)}/T_{\text{sft}}$, the cost is

$$\approx 640N^{(1)}N_{pc}^{(1)}f_{\text{max}} \frac{(\Delta T^{(1)})^2}{T_{\text{sft}}}. \quad (\text{A12})$$

At higher stages, we evaluate the \mathcal{F} -statistic

$$F^{(i-1)} \max \left\{ 1, \frac{N_{pc}^{(i)}}{N_{pf}^{(i-1)}} \right\} \max \left\{ 1, \frac{\Delta T^{(i)}}{\Delta T^{(i-1)}} \right\} N^{(i)} \quad (\text{A13})$$

times, so the operations count is

$$\begin{aligned} & F^{(i-1)} \max \left\{ 1, \frac{N_{pc}^{(i)}}{N_{pf}^{(i-1)}} \right\} \max \left\{ 1, \frac{\Delta T^{(i)}}{\Delta T^{(i-1)}} \right\} \\ & \times \left[\frac{640N^{(i)}\Delta T^{(i)}}{T_{\text{sft}}} \right]. \end{aligned} \quad (\text{A14})$$

[1] P.R. Brady, T. Creighton, C. Cutler, and B.F. Schutz, *Phys. Rev.* **D57** 2101 (1998).

[2] P.R. Brady and T. Creighton, *Phys. Rev.* **D61**, 082001

(2000).

[3] P. Jaranowski, A. Królak, and B.F. Schutz, *Phys. Rev.* **D58** 063001 (1998).

- [4] B. Abbott et al. (The LIGO Scientific Collaboration), *Phys. Rev.* **D69**, 082004 (2004).
- [5] R. Prix and Y. Itoh, [gr-qc/0504006](https://arxiv.org/abs/gr-qc/0504006).
- [6] B. Krishnan, A.M. Sintes, M.A. Papa, B.F. Schutz, S. Frasca, and C. Palomba, *Phys. Rev.* **D70**, 082001 (2004).
- [7] The software can be found on the following websites: <http://www.lsc-group.phys.uwm.edu/daswg/projects/lal.html> and <http://www.lsc-group.phys.uwm.edu/daswg/projects/lalapps.html>
- [8] B. Owen, *Phys. Rev.* **D53**, 6749 (1996).
- [9] J.H. Conway and N.J.A. Sloane, *Sphere Packings, Lattices and Groups*, Springer (1991).
- [10] P. Astone, K.M. Borkowski, P. Jaranowski, and A. Królak, *Phys. Rev.* **D65** 042003 (2003).
- [11] N. Metropolis, A. Rosenbluth, M. Rosenbluth, A. Teller, E. Teller, *J. Chem. Phys.* **21**, 1087 (1953).
- [12] S. Kirkpatrick, C.D. Gelatt Jr., and M.P. Vecchi, *Science* **220**, No. 4598, 671 (1983).
- [13] J.A. Nelder and R. Mead, *Comput. J.* **7**, 308-313, 1965.
- [14] W.H. Press, *Numerical Recipes in C*, Cambridge University Press (2002).
- [15] <http://www.gnu.org/software/gsl/>.
- [16] S.V Dhurandhar and A. Vecchio, *Phys. Rev.* **D63** 122001 (2001).
- [17] <http://www.physics2005.org/events/einsteinathome/#einsteinathome>
- [18] J. R. Gair, L. Barack, T. Creighton, C. Cutler, S. L. Larson, E. S. Phinney, and M. Vallisneri, Proceedings of the Eighth GWDAW Meeting (Milwaukee, 2003); [gr-qc/0405137](https://arxiv.org/abs/gr-qc/0405137).
- [19] Of course an actual search should must take into account the so-called Einstein and Shapiro delays, but these are unimportant for the question of how the search is most efficiently *organized*, which is the focus of this paper.
- [20] An exception is a search for old pulsars presented in tables VII and VIII, where the cost for the follow-up stage turns out to be non-negligible. This example in particular will have to be revisited when better formulas for N_p are available.
- [21] Strictly speaking, Eq. (30) for the number of templates is valid only for observation times which are significantly less than a year. However, unless the discrepancy is many orders of magnitude, the numbers obtained show that it is obviously sufficient for the purposes of this argument.
- [22] Of course, no sensible person would ever claim that he or she had detected a GW pulsar with FA probability of less than 10^{-284} . In such a case, the “statistical error” is so ridiculously small that the true FA rate is dominated by the other, hard-to-quantify factors, such as the probability of having some bug in the instrumentation or in the data analysis code.